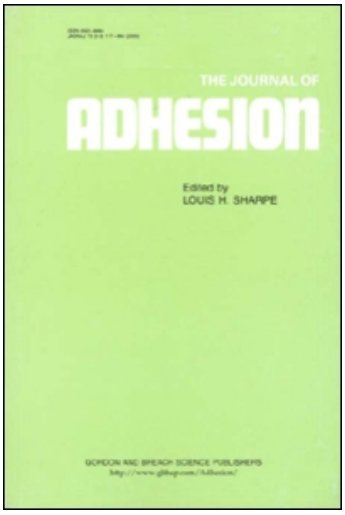

The Journal of Adhesion
Publication details, including instructions for authors and subscription information:
http://www.informaworld.com/smpp/title~content=t713453635

A Comparison of Energy Release Rates in Different Membrane Blister and Peel Tests

Yeh-Hung Lai[ab]; David A. Dillard[a]
[a] Engineering Science and Mechanics Department, Virginia Polytechnic Institute and State University, Blacksburg, VA, USA [b] Eastman Kodak Company, Rochester, NY, U.S.A.

To cite this Article Lai, Yeh-Hung and Dillard, David A.(1996) 'A Comparison of Energy Release Rates in Different Membrane Blister and Peel Tests', The Journal of Adhesion, 56: 1, 59 — 78
To link to this Article: DOI: 10.1080/00218469608010499
URL: http://dx.doi.org/10.1080/00218469608010499

J. Adhesion, 1996, Vol. 56, pp. 59–78
Reprints available directly from the publisher
Photocopying permitted by license only

A Comparison of Energy Release Rates in Different Membrane Blister and Peel Tests

YEH-HUNG LAI* and DAVID A. DILLARD**

Engineering Science and Mechanics Department, Virginia Polytechnic Institute and State University, Blacksburg, VA 24061-0219, USA

(Received October 6, 1994; in final form August 30, 1995)

The relationship between energy release rates and coating stresses in various coating adhesion fracture tests is investigated. In spite of the apparent difference in test geometries and loading conditions, an equivalent peel test can be found for each of the membrane peeling tests examined in this paper. The results suggest that these tests and other membrane peeling tests are special cases of the peel test if examined near the debond front. In addition to clarifying the relationship between peel tests and other membrane peeling tests, the limitations of all possible membrane peeling test geometries with coatings having a tensile prestress are investigated through the study of the fracture efficiency parameter for the most general coating peeling problem. The results suggest that developing high fracture efficiency tests for coating adhesion measurement seems unlikely.

KEY WORDS: Peel test; blister test; energy release rate; fracture mechanics; fracture efficiency; coating; membrane; fracture mechanics.

INTRODUCTION

Coatings of many different types are critical to the successful fabrication and utilization of many manufactured products. Although seldom considered as structural materials, failure of coatings by cracking, fretting, abrasion, and debonding can lead to component failure. A wide variety of qualitative tests for measuring coating performance have been devised. Quantitative tests for measuring adhesion, however, have been quite elusive because the energy required to debond coatings often exceeds the energy required to fracture thin coatings and films. Over the years, a large number of test geometries have been devised for evaluating coating adhesion. One common test which has been used in a variety of configurations is the peel test. In a peel test, a thin, flexible strip is pulled away at some angle from the underlying substrate to which it is adhered. The force required to separate the flexible strip from the substrate, called the peel force, is related to the bond fracture strength and has been used to compare and develop adhesives, conduct quality control, and test surface preparation.[1] Other variations of peel tests include the symmetric peel test[2] and the pull-off test.[3]

Spies[4] was the first to present a theoretical analysis of the mechanics of elastic peeling. He considered 90° peeling of a thin strip and represented the bonded part of the

* Present address: Eastman Kodak Company, Rochester, NY 14650-2116, U.S.A.
** To whom correspondence should be addressed.

strip as an elastic beam on an elastic foundation and the flexible part as an elastica. Similar elastic models have also been obtained by others.[5–7] The mode mixity of peel tests with various peel angles was investigated by Thouless and Jensen.[8] Although the peel test offers a simple test geometry for measuring bond fracture strength, it suffers from several problems. The most severe one is that if the coating is very thin and the adhesion is strong, the coating may tear due to the high membrane/bending stresses or the high stress concentration at the grip. Without plastic/viscoelastic deformation, the peel force is a direct measure of the bond fracture strength. However, when plastic deformation takes place, the plastic dissipation should be considered. Kim *et al.*[9,10] derived the moment-curvature relation for pure bending of an elastoplastic beam and related the experimentally measured peel force to the coating adhesion. They showed that the measured peel force could be two orders of magnitude higher than the actual debond energy when plastic dissipation in the adherends occurred.

Another type of membrane peeling test, the blister test, offers an alternative to the peel tests because the loading method does not require mechanical contact and therefore, eliminates the stress concentration problem associated with gripping a peel specimen. Blister specimens consist of a layer of material adhering or bonded to a substrate except for an initial debonded portion where loading is applied, often by means of a pressurized medium. Over the years, many blister configurations have been proposed. These include Dannenberg's blister,[11] standard (circular) blister,[12–14] constrained blister test,[15–17] island blister,[18,19] and peninsula blister tests.[20,21]. The relatively large number of blister variations is partially attributable to the search for tests to debond the coating without rupturing the coating.

Despite the apparent differences in test geometries and loading conditions between peel tests and blister tests, one can not differentiate between the two tests if the region very near the debond front is examined. One of the objectives of this paper is to clarify whether the peeling mechanisms of blister tests are indeed as different from the peel test as the overall test geometry and the loading condition may suggest, or if they are simply special types of peel tests, as the similarity near the localized debond region may suggest. One peel test variation and three blister goemetries will be compared with peel tests of arbitrary peel angles. The other objective of this paper is to examine whether one can design a coating peeling specimen to achieve a high energy release rate while inducing only small stresses in the specimen, so that yielding or rupture is less likely to occur. To achieve this objective, a general coating peeling specimen with a tensile prestress will be investigated, based on a simple parameter called the fracture efficiency parameter.[22,23]

ENERGY RELEASE RATE OF THE PEEL TEST

Since various membrane peeling tests with prestresses will be compared with the peel test, the energy release rate of the peel test in a thin coating with prestresses will be derived in this section. Consider the peel geometry in Figure 1 where a coating is subjected to an applied peel stress of σ_∞ and an applied peel angle of θ_∞. The bending rigidity of the coating is assumed to be very small so that the membrane solution is applicable. The membrane has a thickness of h and prestrains of ε_0^ξ and ε_0^η, where, as

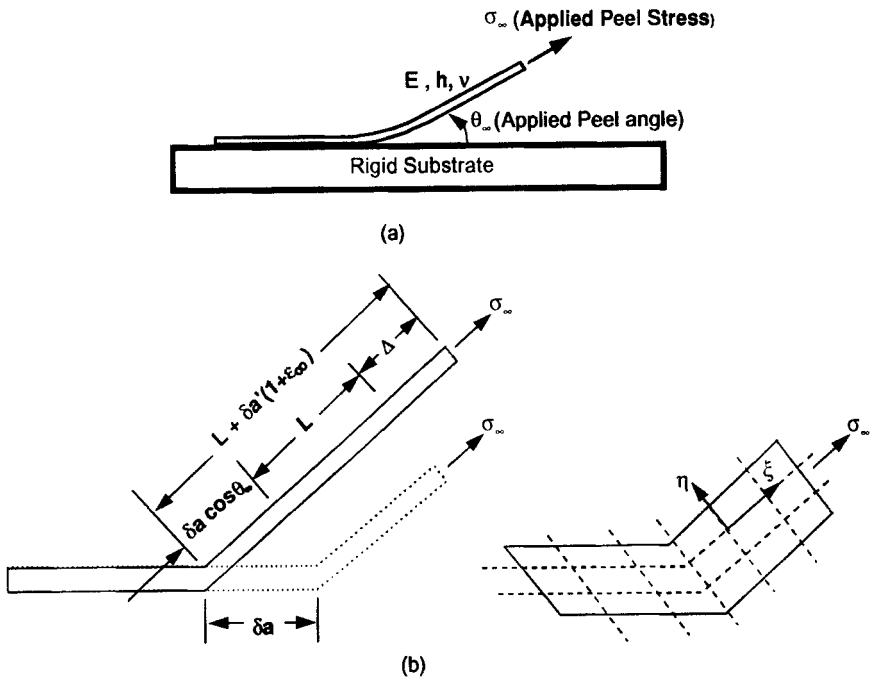

FIGURE 1 Illustration of (a) a peel test and (b) mechanics of peeling.

shown in Figure 1(b), ξ and η represent the directions of the curvilinear coordinates in the membrane surface, with η being the direction parallel to the debond front and ξ being the direction perpendicular to η. Assuming that the inelastic energy dissipation is negligible, the energy release rate can be obtained based on the energy balance consideration:

$$G = \frac{\delta W}{\partial A} - \frac{\delta U}{\partial A} \tag{1}$$

where δW is the change of the external work, δU is the change of the strain energy, and δA is the increment of debonding area, which is expressed as

$$\delta A = b\delta a' \tag{2a}$$

b is the width of the coating strip, and $\delta a'$ is the length of debonded coating at the stress-free state.

It should be noted that δA may also be taken with respect to the substrate surface:

$$\delta A = b\delta a \tag{2b}$$

where $\delta a = \delta a'(1 + \varepsilon_0^{\xi})$.

Since Thouless and Jensen[24] have found that the energy release rate obtained based on Eq. (2a) is more consistent with that obtained from the stress intensity factors, Eq. (2a) will be used to derive the energy release rate derived in this paper.

From Figure 1(b), the change of the external work can be expressed as

$$\delta W = \sigma_\infty bh\Delta = \sigma_\infty bh[\delta a'(1+\varepsilon_\infty) - \delta a\cos\theta_\infty]$$
$$= \sigma_\infty bh\delta a'[(1+\varepsilon_\infty) - (1+\varepsilon_0^\xi)\cos\theta_\infty] \tag{3}$$

where ε_∞ is the applied peel strain.

The determination of δU is somewhat more complicated. It depends on the condition of the prestrain ε_0^η in the debonded portion of the membrane. Two possible types are considered in this paper. Type I considers that ε_0^η in the debonded region is equal to that in the bonded region, which might be appropriate for a very wide specimen, or one in which the two sides of the membrane are constrained in the η direction. Type II represents the case in which ε_0^η in the debonded region is released and becomes zero. Therefore, δU is expressed by:

Type I: $$\delta U = \frac{bh}{2}\delta a'(\sigma_\infty\varepsilon_\infty - \sigma_0^\xi\varepsilon_0^\xi) \tag{4a}$$

Type II: $$\delta U = \frac{bh}{2}\delta a'(\sigma_\infty\varepsilon_\infty - \sigma_0^\xi\varepsilon_0^\xi - \sigma_0^\eta\varepsilon_0^\eta) \tag{4b}$$

From Eqs. (1) to (4) the energy release rate can be obtained as:

Type I: $$G = \sigma_\infty h\left[1 + \frac{\varepsilon_\infty}{2} - \varepsilon_0^\xi\cos\theta_\infty - \cos\theta_\infty\right] + \frac{h\sigma_0^\xi\varepsilon_0^\xi}{2} \tag{5a}$$

Type II: $$G = \sigma_\infty h\left[1 + \frac{\varepsilon_\infty}{2} - \varepsilon_0^\xi\cos\theta_\infty - \cos\theta_\infty\right] + \frac{h}{2}(\sigma_0^\xi\varepsilon_0^\xi + \sigma_0^\eta\varepsilon_0^\eta) \tag{5b}$$

Since no constitutive equations are used in the derivation up to this point, the solutions can be considered as general solutions for peel tests in plane problems. In the following sections, several special cases of interest to the current study will be discussed.

When the coating is not prestressed, Eqs. (5) become the familiar peeling equation:[25]

$$G = \sigma_\infty h\left[1 + \frac{\sigma_\infty}{2\hat{E}} - \cos\theta_\infty\right] \tag{6}$$

where $\hat{E} = E$ for the plane stress case, $\hat{E} = (E/(1-\nu^2))$ for the plane strain case, and E and ν are the Young's modulus and Poisson's ratio of the membrane, respectively. When the coating is subjected to a uni-axial prestress, were $\varepsilon_0^\xi = \varepsilon_0 = (\sigma_0/\hat{E})$ and $\varepsilon_0^\eta = 0$, Eqs. (5) become

$$G = \sigma_\infty h\left[1 + \frac{\sigma_\infty}{2\hat{E}} - \frac{\sigma_0}{\hat{E}}\cos\theta_\infty - \cos\theta_\infty\right] + \frac{h\sigma_0^2}{2\hat{E}} \tag{7}$$

Equation (7) is the same as that derived by Thouless and Jensen.[24]

Perhaps the most frequently encountered peeling situation involves a coating subjected to an equal bi-axial prestress, where the prestresses and prestrains can be expressed as

$$\varepsilon_0^\xi = \varepsilon_0^\eta = \varepsilon_0, \quad \sigma_0^\xi = \sigma_0^\eta = \sigma_0, \quad \text{and} \quad \varepsilon_0 = \frac{1-\nu}{E}\sigma_0 \tag{8}$$

In this case, the energy release rate can be expressed as:

$$\text{Type I:} \qquad G = \sigma_\infty h\left[1 + \frac{\sigma_\infty}{2\hat{E}} - \frac{1-\nu}{E}\sigma_0 \cos\theta_\infty - \cos\theta_\infty\right] + \frac{h(1-\nu)}{2E}\sigma_0^2 \tag{9a}$$

$$\text{Type II:} \qquad G = \sigma_\infty h\left[1 + \frac{\sigma_\infty}{2\hat{E}} - \frac{1-\nu}{E}\sigma_0 \cos\theta_\infty - \cos\theta_\infty\right] + \frac{h(1-\nu)}{E}\sigma_0^2 \tag{9b}$$

It is interesting to note that the last term in Eq. (9b) is twice the corresponding one in Eq. (9a).

MEMBRANE PEELING TEST COMPARISON

As an illustration of how other membrane peeling configurations compare to the peel test, several membrane peeling configurations with different test geometries and loading conditions will be chosen. These configurations include the pull-off, one-dimensional blister, standard blister, and island blister tests, as shown in Figure 2.

Peel Test and Pull-Off Test Comparison

In this section, the peel test (Fig. 1(a)) and one of its variations, the pull-off test[3] (Fig. 2(a)) are compared. For all cases, it is assumed that the coating is loaded within the elastic range and the substrate is rigid. The energy release rate for the pull-off test was obtained by Gent and Kaang[3] as

$$G = \frac{3}{8}\frac{F\theta}{w} \tag{10}$$

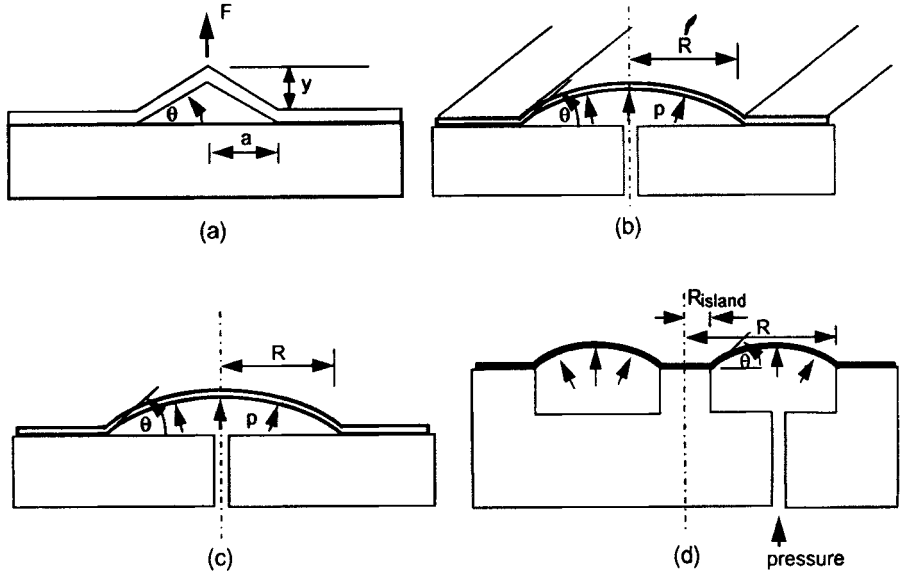

FIGURE 2 Illustration of (a) pull-off test, (b) one-dimensional blister test, (c) standard circular blister test, and (d) island blister test.

where F is the pull-off force, θ is the membrane peel angle, and w is the width of the adherend.

Equation (10) was derived based on the assumption of a small membrane peel angle, which can be easily re-written as

$$G = \frac{3\sigma^2 h}{2\hat{E}} \tag{11}$$

where σ is the membrane peel stress, which is defined as the membrane stress in the direction with an angle θ to the substrate.

From Eqs. (6), for given material properties and specimen thickness, both the applied peel stress and peel angle are independent variables in determining the energy release rate of the peel test. However, one can not control the membrane peel stress and angle independently in a pull-off test in which these two quantities are interdependent.

Since the applied peel stress and peel angle in a peel test can be chosen arbitrarily, we may choose the applied peel stress and applied peel angle to be exactly the same as the membrane peel stress and membrane peel angle, respectively, in the pull-off test. The peel and pull-off tests of the same peel stress and peel angle should give the same stress state in the specimen away from the point where the load is applied; therefore, they should produce the same energy release rate as will be proved as follows.

From the pull-off test, we have the relation

$$\cos\theta = \frac{1}{1+\varepsilon} = 1 - \varepsilon + \frac{\varepsilon^2}{2} - \cdots \tag{12}$$

where ε is the membrane peel strain.

Substituting the above relation into Eq. (6), and letting $\sigma_\infty = \sigma$ and $\theta_\infty = \theta$, we can obtain the energy release rate for the peel test with the same membrane peel stress and angle as the pull-off test:

$$G = \sigma h\left(1 + \frac{\varepsilon}{2} - 1 + \varepsilon - \frac{\varepsilon^2}{2} + \cdots\right) \tag{13}$$

Assuming the strain is small, we may neglect the higher order strain terms and obtain

$$G = \frac{3\sigma^2 h}{2\hat{E}} \tag{14}$$

which is exactly the same as Eq. (11) for the pull-off test. The agreement between Eqs. (11) and (14) shows that for given membrane peel stress and angle, the pull-off test and peel test should produce the same energy release rate.

This example suggests that in spite of the difference in the test geometry and the applied load for pull-off and peel tests, the energy release rates are the same for given membrane peel stress and peel angle. In the next section, an idealized plane blister, the one-dimensional blister (Fig. 2(b)), is compared with the equivalent peel test.

Peel Test and One-Dimensional Blister Configuration Comparison

In the vicinity of the debond front for any peel test, some distance is required for the stress in the ξ direction to change from the direction of the applied peel stress to that of

the bonded surface. If the thickness of the membrane is infinitesimally small, this distance will approach zero. For the current comparison between the peel test and one-dimensional blister test for thin membranes, it is assumed that this distance is negligible so that the membrane stress in the ξ direction and the take-off angle, or the membrane peel angle, at the boundary could be chosen and used as the applied peel stress and the peel angle in the equivalent peel test. This is consistent with the assumption that the peeled adherend can be modeled as a membrane.

The solution for the one-dimensional membrane blister is given in the Appendix A. For simplicity, only the case of plane strain without prestress will be discussed. The energy release rate for the one-dimensional blister test can then be expressed as

$$G = \frac{7}{12}[6(1-\nu^2)]^{1/3}\frac{(pR)^{4/3}}{(Eh)^{1/3}} \tag{15}$$

where R is half of the debond width, and p is the applied pressure.
Alternately, G can also be expressed in terms of the membrane peel stress as

$$G = \frac{7\sigma^2 h}{2E} \tag{16}$$

From Eqs. (A.4b), (A.4d), and (A.6a) and letting σ be the outermost membrane stress, the tangent of the membrane peel angle can easily be obtained as:

$$\tan\theta = (6\sigma/E)^{1/2} \tag{17}$$

and the cosine of the membrane peel angle is given as

$$\cos\theta = (1+6\sigma/E)^{-1/2} = 1 - \frac{6\sigma}{2E} + \frac{3}{8}\left(\frac{6\sigma}{E}\right)^2 - \cdots \tag{18}$$

Substituting the above equation into Eq. (6) and neglecting the higher order strain terms, we can obtain the energy release rate for the peel test with the same membrane peel stress and peel angle at the debond front as the one-dimensional blister test:

$$G = \frac{7\sigma^2 h}{2E} \tag{19}$$

The Eqs. (19) and (6) are exactly the same, which indicates that the one-dimensional blister test and peel test give the same energy release rate under the same membrane peel stress and peel angle, despite the very different loading method and deformed shape of the specimens away from the debond front.

Comparison between the Peel Test and Circular Blister Tests

Two circular blisters are compared with the peel test in this paper – the standard blister (Fig. 2(c)) and the island blister (Fig. 2(d)). In the comparison of the pull-off/peel configurations and the one-dimensional blister/peel configurations, only the plane problem was considered. In order to compare the peel test and circular blister tests following a similar procedure, we need to consider whether the membrane peel stress and angle obtained in a axisymmetric membrane problem can be used in a plane membrane peel problem.

For a plane strain membrane problem with an equal bi-axial prestress, the stress state in the membrane is given by:

$$\sigma_\eta = \nu\sigma_\xi + (1-\nu)\sigma_0 \tag{20}$$

In an axisymmetric problem, the meridian and circumferential stresses do not obey a simple relationship as in Eq. (20). Therefore, the stress state in the plane and axisymmetric problems are different. However, **at the boundary**, the circumferential strain ε_θ is zero. Thus, the meridian and circumferential stresses obey an identical relationship:

$$\sigma_\theta = \nu\sigma_r + (1-\nu)\sigma_0 \tag{21}$$

where subscript r represents the meridian direction, and subscript θ represents the circumferential direction.

In spite of the obvious difference between the solutions for the plane strain and axisymmetric problems, these two problems should have the same stress state at the boundary if the meridian stress and the prestress in the axisymmetric and plane strain problems are taken to be equal there.

Following the same argument made in the previous section, the distance for the direction of the meridian stress to change from that of the take-off angle at the debonded side to that of the bonded surface is assumed to be negligible. Since the stress state of an axisymmetric membrane problem would approach that of a plane strain problem as the point of interest approaches the boundary from the membrane at the debonded side, the meridian stress and take-off angle at the boundary of the circular blisters could be taken as the applied membrane peel stress and peel angle in the equivalent peel tests.

The tangent of the membrane peel angle at the boundary for the circular blister is given by:

$$\tan\theta = \frac{dw}{dr} = \frac{dw}{R\,dx} = \frac{d\bar{w}}{dx}\left(\frac{pR}{Eh}\right)^{1/3} = m\left(\frac{pR}{Eh}\right)^{1/3} \tag{22a}$$

where

$$m = \frac{d\bar{w}}{dx} \tag{22b}$$

From Eqs. (22) and (A.4d), the cosine of the membrane peel angle is given by:

$$\cos\theta = \frac{1}{\left[1+\dfrac{m^2\sigma}{\bar{\sigma}E}\right]^{1/2}} = 1 - \frac{1}{2}\left(\frac{m^2\sigma}{\bar{\sigma}E}\right) + \frac{3}{8}\left(\frac{m^2\sigma}{\bar{\sigma}E}\right)^2 - \cdots \tag{23}$$

where $\sigma = \sigma_r(R)$ and $\bar{\sigma} = \bar{\sigma}_r(1)$ for the standard blister, and $\sigma = \sigma_r(R_{\text{island}})$ and $\bar{\sigma} = \bar{\sigma}_r(a)$ for the island blister, where a is the nondimensional island radius as defined in Eq. (A.19).

It should be noted that the above quantities are evaluated at outer and inner boundaries for the standard blister and island blister, respectively. By substituting Eq. (23) and membrane stress at the debond front into Eq. (9a), we can obtain the energy release rate of the equivalent peel test which has the same peel angle and

membrane peel stress as those at the debond front of the circular blister tests:

$$G = \sigma h \left\{ 1 + \frac{(1-\nu^2)}{2E}\sigma - \frac{(1-\nu)}{E}\sigma_0 \left[1 - \frac{1}{2}\left(\frac{m^2\sigma}{\bar{\sigma}E}\right) + \frac{3}{8}\left(\frac{m^2\sigma}{\bar{\sigma}E}\right)^2 - \cdots \right] \right.$$
$$\left. - 1 + \frac{1}{2}\left(\frac{m^2\sigma}{\bar{\sigma}E}\right) - \frac{3}{8}\left(\frac{m^2\sigma}{\bar{\sigma}E}\right)^2 + \cdots \right\} + \frac{(1-\nu)h}{2E}\sigma_0^2 \tag{24}$$

Assuming the strain is small, we may neglect the higher order strain terms in Eq. (24) and obtain the ratio of the energy release rate to the square of membrane peel stress at the debond front:

$$\frac{G}{\sigma^2} = \frac{h}{E}\left[\frac{(1-\nu^2)}{2} + \frac{1}{2}\left(\frac{m^2}{\bar{\sigma}}\right) - (1-\nu)\frac{\bar{\sigma}_0}{\bar{\sigma}} + \frac{(1-\nu)}{2}\frac{\bar{\sigma}_0^2}{\bar{\sigma}^2} \right]. \tag{25}$$

It should be noted that since in blister tests the prestress in the η direction is not released in the debonded region, Eq. (9a) for the energy release rate in the Type I of peel test is used. When the prestress in the η direction can be released in the debonded region, as is more realistic experimentally in a peel test, the ratio of the energy release rate to the square of membrane peel stress at the debond front is expressed as:

$$\frac{G}{\sigma^2} = \frac{h}{E}\left[\frac{(1-\nu^2)}{2} + \frac{1}{2}\left(\frac{m^2}{\bar{\sigma}}\right) - (1-\nu)\frac{\bar{\sigma}_0}{\bar{\sigma}} + (1-\nu)\frac{\bar{\sigma}_0^2}{\bar{\sigma}^2} \right] \tag{26}$$

Eqs. (25) and (26) will be evaluated numerically in the following discussions.

Figure 3 illustrates the ratio of the energy release rate to the square of the membrane peel stress *versus* the nondimensional prestress in a standard blister test. A typical Poisson's ratio of 0.3 is used. Excellent agreement is seen between the standard blister and the equivalent peel tests. The ratio decreases as the prestress increases and is expected to approach zero when the prestress is very large. It is interesting to note that when the prestress in the η direction is allowed to be released (Type II), the energy release rate is larger than the blister test and its equivalent peel test (Type I) for a given membane peel stress. The deviation increases as the nondimensional prestress increases. When the nondimensional prestress is 1, the deviation is larger than 500%. The results suggest that in a low angle peel test it is important to account for the contribution of prestresses properly.

Figure 4 illustrates the ratio of the energy release rate to the square of the membrane peel stress *versus* the nondimensional island radius in an island blister test with different nondimensional prestresses. The Poisson's ratio is 0.3. For the cases with small nondimensional prestress, such as the one with zero prestress in Figure 4, the ratio increases as the island radius increases, while the ratio decreases for larger prestress cases. For the case of relatively large nondimensional prestress, the ratio approaches zero as seen in the cases with nondimensional prestress of 3 and 8. Excellent agreement is also seen between the island blister and peel test results for all prestresses and sland radii. It should also be noted that it is expected that the island blister test and its equivalent peel test of Type I should give a lower energy release rate than the more realistic peel test of Type II for a given membrane peel stress when prestress is high.

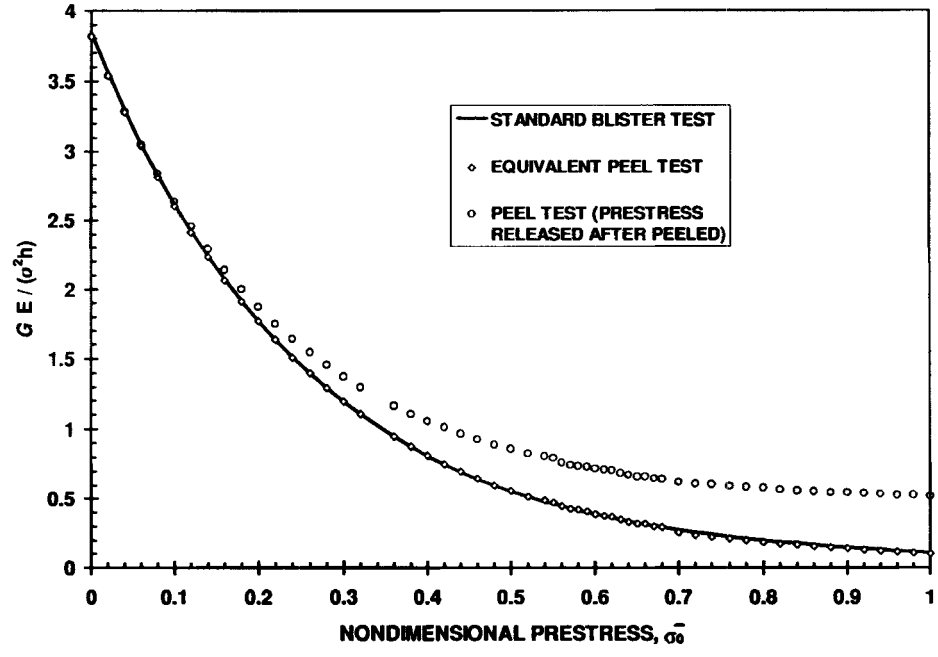

FIGURE 3 Ratio of energy release rate to the square of membrane peel stress *versus* nondimensional prestress in a standard blister test. Poisson's ratio is 0.3.

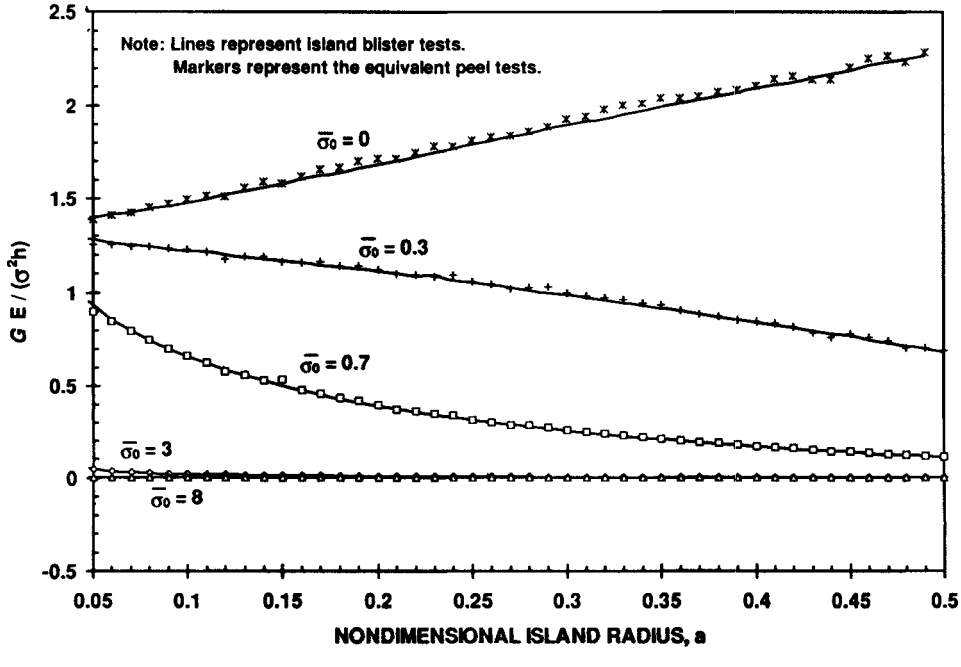

FIGURE 4 Ratio of energy release rate to the square of membrane peel stress *versus* nondimensional island radius in an island blister test with different nondimensional prestresses. Poisson's ratio is 0.3.

Although the four membrane peeling configurations discussed so far are all special cases of the peel test if examined near the debond front, each produces a different energy release rate for the same membrane peel stress because the peel angles are not the same.

THE FRACTURE EFFICIENCY FOR THE MOST GENERAL COATING PEELING PROBLEM

In this section, the variation of the energy release rate of the general coating peeling tests will be investigated. Because most analysis methods for coating adhesion tests are based on the assumption that the coating is loaded within the elastic range, it is important to know whether the maximum stress has exceeded the yield stress upon debonding. It should be noted that within the framework of linear elastic fracture mechanics (LEFM), small scale yielding at the crack tip is allowed. In this paper, the specimen is considered grossly yielded when the maximum non-singular stress exceeds the yield strength of the coating.

In this section, instead of investigating a limited number of membrane peeling configurations, a general coating peeling problem as shown in Figure 5 is considered. In this problem, a coating is adhering to a substrate with a bending rigidity much larger than the coating and is subjected to a combined loading of axial force and bending moment. According to Hutchinson and Suo[26] the energy release rate is given by

$$G = [(P - \sigma_0 h)^2 + 12M^2/h^2]/2\hat{E}h \tag{27}$$

where P is the resultant in-plane stress per unit width in the coating at the debonded side, and M is the bending moment per unit width. Since P and M can be applied independently, one may change the loading conditions among various membrane peeling tests, and even plate-like peel or blister tests, by changing the ratio between P and M. With known P and M, the maximum non-singular stress can be easily obtained. Alternately, if the resultant in-plane stress, prestress, and energy release rate are known, as are the cases discussed in the previous sections, the bending moment at the debond front could be easily obtained using Eq. (27). This method has been employed by Thouless and Jensen to determine the bending moment in a peel test.[8] Thouless and

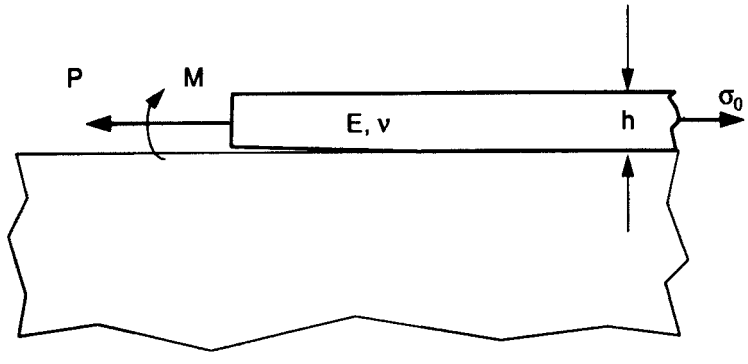

FIGURE 5 Illustration of the general coating delamination problem.

Jensen have also suggested adding a shear force term in Eq. (27) as a correction term for the peel geometry. However, based on Appendix B, in which the relative contributions of axial force, shear force, and bending moment to the energy release rate are studied, it is concluded that the shear force term could be neglected except when the applied peel strain is very large and the peel angle approaches 90°.

To study the relationship between the energy release rate and the maximum non-singular stress, it is convenient to use a simple quantity called the fracture efficiency parameter[23,24] which is defined as

$$T_e = \frac{G}{\sigma_{\max}^2} \tag{28}$$

where $\sigma_{\max}$ is the maximum non-singular stress, which is generally obtained from a mechanics of materials solution.

The fracture efficiency parameter is an index of fracture efficiency. A test design with a high fracture efficiency is more likely to cause debond without yielding or rupturing. Alternately, yielding is more likely to occur if the fracture efficiency is low and, therefore, the measured bond fracture strength may be in error if yielding is not properly accounted for. By comparing the fracture efficiency parameter among different test configurations, one can determine an appropriate specimen design to reduce the likelihood of yielding.

For the general coating peeling specimen, the fracture efficiency parameter is given by

$$T_e = \min\left\{ \frac{h}{\hat{E}} \frac{\left(1-\frac{\sigma_0 h}{P}\right)^2 + 12\left(\frac{M}{Ph}\right)^2}{2\left(\left|\frac{6M}{Ph}\right|+1\right)^2}, \quad \frac{h}{\hat{E}} \frac{\left(1-\frac{\sigma_0 h}{P}\right)^2 + 12\left(\frac{M}{Ph}\right)^2}{2\left(\frac{\sigma_0 h}{P}\right)^2} \right\} \tag{29}$$

From Eq. (29), the fracture efficiency parameter is a function of three variables, the normalized moment, M/Ph, the normalized prestress, $\sigma_0 h/P$, and the thickness to modulus ratio, $h/\hat{E}$. It should be noted that it has been assumed that the maximum stress is located at the debond front in the following dicusssions.

Figure 6 illustrates the nondimensional fracture efficiency parameter, $T_e\hat{E}/h$, *versus* normalized moment for the general coating peeling problem with various normalized prestresses. The results in this figure cover all possible results for membrane peeling configurations with a tensile coating prestress. The case with a normalized prestress of 1 corresponds to specimens with such a high prestress that the stress induced by the external load is negligible compared with the prestress. When the prestress is zero, the maximum nondimensional fracture efficiency parameter of 0.5 is found at zero moment. As the normalized moment increases from zero, the fracture efficiency decreases and reaches a constant of 0.167 of the nondimensional fracture efficiency parameter at very large normalized moments. When the normalized prestress is 1, the minimum nondimensional fracture efficiency parameter of 0 is found at zero moment. As the normalized moment increases, the nondimensional fracture efficiency parameter increases. The curves with normalized prestresses of 0 and 1 are the two extreme

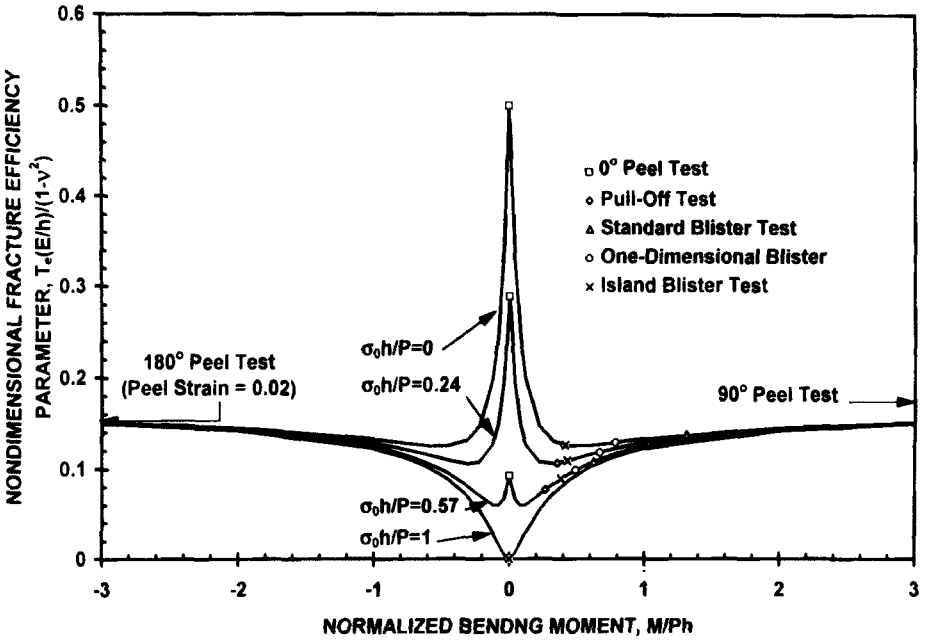

FIGURE 6 Nondimensional fracture efficiency parameter *versus* normalized moment for various membrane peeling tests.

solutions. Other curves with a normalized prestress between 0 and 1 should locate between these two curves.

Figure 6 also illustrates several typical membrane peeling tests for coatings with a tensile prestress. Peel tests of 0°, 90°, and 180° peel angles and membrane peeling tests such as standard blister, island blister with a nondimensional island radius of 0.1, one-dimensional blister, and pull-off test are also marked in this figure. Since the energy release rate and membrane peel stress are readily obtained in the previous section and Appendix A, the moment can be easily determined using Eq. (27). In these tests, the 0° peel test with a coating of zero prestress has the highest fracture efficiency parameter of 0.5, which is also the highest in all possible tests with a normalized prestress in the range of 0 and 1. As the prestress increases, the nondimensional fracture efficiency parameter decreases. When the applied peel stress is equal to the prestress in the 0° peel test, the energy release rate is equal to zero and, therefore, the fracture efficiency parameter is zero. It is also interesting to see that in the zero prestress case, the pull-off, one-dimensional blister, island blister, and standard blister tests have similar nondimensional fracture efficiency parameters. As the normalized prestress increases, the fracture efficiency of these three tests decreases and then approaches zero when the normalized prestress approaches 1. The results in Figure 6 suggest that when the prestress is very small, peel tests with very small angles may be preferable. However, when the prestress is relatively large, a high-angle peel test may be preferable.

Despite several advantages over the peel tests, it is found that the blister test is more likely to initiate yielding at the debond front compared with the 90° and 180° peel tests. It should be noted that significant curl-up and, therefore, bending-induced yielding, in a peeled sample from a 90° or 180° peel test is often observed, but not in a blister test. One should not be misled by this observation to conclude that blister tests are less likely to initiate yielding than a 90° or 180° peel test. In a high-angle peel test, the significant curl-up is mostly due to high bending stress, while in low-angle peel tests such as the blister test, the yielding is due to the combination of membrane and bending stress and, therefore, may result in less curl-up. Once the yielding occurs, one should use the appropriate plastic analysis to assess the extent of the yielding and determine the proper energy release rate.

It is seen from the results in Figure 6 that, since the existing membrane peeling test configurations can cover the entire range of fracture efficiency parameter when normalized prestress is between 0 and 1, it is unlikely for one to develop new membrane peeling tests with higher fracture efficiency. It should be noted that the effect of the fracture mode mixity is not considered in this paper although a recent study suggests that it may have a significant effect on the measured bond fracture strength.[26] Further study of the fracture efficiency is needed to assess the effect of the fracture mode. To avoid the error caused by yielding, one may need to increase the coating thickness significantly, to use a backing on top of the coating, or to analyze the experimental results using an elastic-plastic solution.

CONCLUSIONS

The peeling mechanism of several coating adhesion measurement techniques was investigated by considering the relationship between energy release rates and coating stresses. Specifically, five membrane peeling configurations, the peel test, pull-off test, one-dimensional blister, standard blister, island blister, and the general coating peeling problem were investigated. In spite of the different test geometries and loading conditions, the pull-off, one-dimensional blister, standard blister, and island blister configurations were all found to be special cases of the peel test if examined near the debond front. Each test produces the same energy release rate as the peel test if subjected to the same membrane peel stress and peel angle. Although only four membrane peeling configurations were compared with the peel test in this paper, the results suggest that other membrane peeling tests should also be the special cases of the peel tests.

In addition to clarifying the relationship between peel tests and other membrane peeling tests, this paper also discussed the limitations of all membranes peeling tests through a study of the fracture efficiency parameter for the general coating peeling problem with a tensile prestress. Defined as the ratio between the energy release rate and the square of the maximum non-singular stress, the fracture efficiency parameter represents how high an energy release rate a certain specimen may produce for a given maximum non-singular stress in the coating. The results suggest that when the prestress is very small, a peel test with very small peel angle may be preferable since it has a relatively high fracture efficiency and, therefore, is less likely to cause yielding or

rupturing. However, when the prestress is relatively large, a peel test with a high peel angle may be a better choice. Since the existing membrane peeling test configurations can cover the entire range of fracture efficiency parameter, it is unlikely that one can develop a new membrane peeling test with a higher fracture efficiency.

Acknowledgements

The authors would like to acknowledge the financial support of the National Science Foundation's Science and Technology Center on High Performance Polymeric Adhesives and Composites at Virginia Tech (Contract DMR 9120004), the Center for Adhesive and Sealant Science at Virginia Tech, and the ALCOA Foundation.

References

1. ASTM, "D1876-72", "D3167-73T", "D903-49", Annual Book of ASTM Standards (1993).
2. A. N. Gent and G. R. Hamed, *J. Appl. Polym. Science* **21**, 2817 (1977).
3. A. N. Gent and S. Y. Kaang, *J. Appl. Polym. Science* **32**, 4689 (1986).
4. G. J. Spies, *J. Aircraft Engineering* **25**, 64 (1953).
5. J. J. Bikerman, *J. Applied Physics* **28**, 1484 (1957).
6. D. H. Kaeble, *Trans. Soc. Rheol.* **3**, 161 (1959).
7. D. W. Nicholson, *Intern. J. Fracture* **13**, 279 (1977).
8. M. D. Thouless and H. M. Jensen, *J. Adhesion* **38**, 185 (1992).
9. K. S. Kim and N. Aravas, *Intern. J. Solids Structures* **24**, 417 (1988).
10. J. Kim, K. S. Kim and Y. H. Kim, *J. Adhesion Sci. Technol.* **3**, 175 (1989).
11. H. Dannenberg, *J. Appl. Polym. Sci.* **5**, 125 (1961).
12. A. N. Gent and L. H. Lewandowski, *J. Appl. Polym. Sci.* **33**, 1567 (1987).
13. M. G. Allen and S. D. Senturia, *J. Adhesion*, **25**, 303 (1988).
14. M. L. Williams, *J. Adhesion* **4**, 307 (1972).
15. D. A. Dillard and Y. S. Chang, *VPI Report #VPI-E--87-24*, Blacksburg, Virginia (1987).
16. Y. S. Chang, Y. H. Lai and D. A. Dillard, *J. Adhesion* **27**, 197 (1989).
17. J. Napolitano, A. Chudnovsky and A. Moet, *J. Adhesion Sci. Technol.* **2**, 311 (1988).
18. M. G. Allen and S. D. Senturia *J. Adhesion* **29**, 219 (1989).
19. M. G. Allen, PhD Dissertation, Massachusetts Institute of Technology (1989).
20. D. A. Dillard, Y. H. Lai, Y. S. Chang, T. Corson and Y. Bao, *Proc. 1990 Society Experimental Mechanics Confernece on Experimental Mechanics*, Albuquerque, New Mexico, June 1990, 575 (1990).
21. D. A. Dillard and Y. Bao, *J. Adhesion* **63**, 253 (1991).
22. Y. H. Lai and D. A. Dillard, *J. Adhesion Sci. Technol.* **8**, 663 (1994).
23. Y. H. Lai and D. A. Dillard, *Intern. J. Solids Structures* (in review)..
24. M. D. Thouless and H. M. Jensen, *J. Adhesion Sci. Technol.* **8**, 579 (1994).
25. G. P. Anderson, K. L. DeVries and M. L. Williams, *Analysis and Testing of Adhesive Bonds* (Academic Press, New York, 1977).
26. J. W. Hutchinson and Z. Suo, *Adv. Appl. Mech.* **29**, 63 (1992).
27. R. Kao and N. Perrone, *Intern. J. Solids Structures* **7**, 1601 (1971).

APPENDIX A: SOLUTIONS OF BLISTER TESTS

The cross section of the membrane blister is shown in Figure A.1. This figure can represent either a plane blister or an axisymmetric blister. This appendix will briefly describe the solutions for the one-dimensional blister, standard blister, and island blister tests.

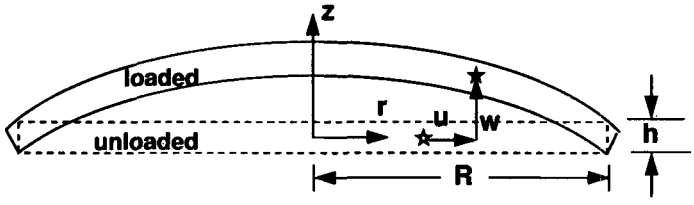

FIGURE A.1 The cross section of a pressurized membrane.

One Dimensional Blister

The one-dimensional blister consists of a membrane bonded along two straight parallel edges. For the plane strain case, the constitutive equation can be found as

$$\sigma_r = \frac{E}{(1-\nu^2)}\varepsilon_r + \sigma_0 \tag{A.1}$$

where σ_0 is the prestress in the membrane, σ_r is the total meridian stress in the membrane and is the sum of the prestress and the stress due to the applied load, and ε_r is the meridian strain in the membrane caused by the applied load. It does not include the strain due to the prestress.

The strain and displacement relationship is given by

$$\varepsilon_r = \frac{du}{dr} + \frac{1}{2}\left(\frac{dw}{dr}\right)^2, \tag{A.2}$$

where u is the displacement in the radial direction, and w is the displacement in the transverse direction.

The equilibrium equation in the meridian direction is

$$\frac{d(\sigma_r h)}{dr} = 0 \tag{A.3a}$$

and the equilibrium equation in the direction normal to the membrane surface is

$$\sigma_r h \frac{d^2 w}{dr^2} = -p \tag{A.3b}$$

where p is the pressure.

It should be noted that, during the derivation of the above equations, large displacement, small rotation and small strain assumptions have been made. By substituting constitutive and strain/displacement relations into the equilibrium equations and introducing the following nondimensional forms,

$$\bar{u} = \frac{u}{R}\left(\frac{pR}{Eh}\right)^{-2/3} \tag{A.4a}$$

$$\bar{w} = \frac{w}{R}\left(\frac{pR}{Eh}\right)^{-1/3} \tag{A.4b}$$

$$\bar{\sigma}_0 = \frac{\sigma_0}{E}\left(\frac{pR}{Eh}\right)^{-2/3} \tag{A.4c}$$

$$\bar{\sigma}_r = \frac{\sigma_r}{E}\left(\frac{pR}{Eh}\right)^{-2/3} \tag{A.4d}$$

and

$$x = \frac{r}{R} \tag{A.4e}$$

we can obtain the following two governing equations for the one-dimensional blister:

$$\bar{u}_{,xx} + \bar{w}_{,x}\bar{w}_{,xx} = 0 \tag{A.5a}$$

and

$$\bar{w}_{,xx}\left(\bar{u}_{,x} + \frac{1}{2}\bar{w}_{,x}^2 + \bar{\sigma}_0(1-\nu^2)\right) = -(1-\nu^2) \tag{A.5b}$$

where the comma denotes partial differentiation with respect to the indices which follow.

By imposing the boundary conditions of $w_{,x} = u = 0$ at $x = 0$ and $w = u = 0$ at $x = 1$, we can solve for w and u as

$$\bar{w}(x) = \frac{c}{2}(x^2 - 1) \tag{A.6a}$$

and

$$\bar{u}(x) = -\frac{c^2}{6}x^3 + \frac{c^2}{6}x \tag{A.6b}$$

and c is expressed as:

$$c = \frac{-2\bar{\sigma}_0(1-\nu^2)}{\{-3(1-\nu^2) + [9(1-\nu^2)^2 + 8\bar{\sigma}_0^3(1-\nu^2)^3]^{1/2}\}^{1/3}} + \{-3(1-\nu^2) + [9(1-\nu^2)^2 + 8\bar{\sigma}_0^3(1-\nu^2)^3]^{1/2}\}^{1/3} \tag{A.7}$$

It is found that, in the case without prestress,

$$c = -[6(1-\nu^2)]^{1/3} \tag{A.8}$$

After the displacements, $\bar{w}(x)$ and $\bar{u}(x)$, are determined, we can easily find the non-dimensional membrane stress, $\bar{\sigma}_r$, given by

$$\bar{\sigma}_r = -\frac{1}{c} \tag{A.9}$$

Based on the energy balance equation,

$$G\delta A = \delta W - \delta U \tag{A.10}$$

where δA is the debonding area, δW is the change in the external work during the debonding process, δU is the change in the strain energy during the debonding process, and assuming that the material is loaded within the elastic range, the energy release rate can be obtained as

$$G=\frac{(pR)^{4/3}}{2(Eh)^{1/3}}\left\{\frac{-2}{9}\left[7c-2\bar{\sigma}_0\frac{dc}{d\bar{\sigma}_0}\right]-\frac{1-\nu^2}{3}\left[7\left(\frac{1}{c^2}-\bar{\sigma}_0^2\right)+4\bar{\sigma}_0\left(\frac{1}{c^3}\frac{dc}{d\bar{\sigma}_0}+\bar{\sigma}_0\right)\right]\right\} \tag{A.11}$$

It is noted that, for the case without prestress, the energy release rate reduces to

$$G=\frac{7}{12}[6(1-\nu^2)]^{1/3}\frac{(pR)^{4/3}}{(Eh)^{1/3}} \tag{A.12}$$

Circular Blister

Following a similar procedure for the one-dimensional blister, the solution and the energy release rate for the standard and island blister tests can be obtained and will be described briefly as follows.

The stress-strain relations are given by

$$\sigma_r=\frac{E}{(1-\nu^2)}(\varepsilon_r+\nu\varepsilon_\theta)+\sigma_0 \tag{A.13a}$$

$$\sigma_\theta=\frac{E}{(1-\nu^2)}(\varepsilon_\theta+\nu\varepsilon_r)+\sigma_0 \tag{A.13b}$$

where σ_θ is the circumferential stress, and ε_θ is the circumferential strain due to the applied load.

The meridian strain is given by Eq. (A.2) and the circumferential strain is given by

$$\varepsilon_\theta=\frac{u+r}{r}-1=\frac{u}{r} \tag{A.14a}$$

Equilibrium equations in the meridian direction and the direction normal to the membrane suface are

$$(r\sigma_r)_{,r}=\sigma_\theta \tag{A.14b}$$

and

$$\frac{1}{r}(r\sigma_r hw_{,r})+p=0 \tag{A.14c}$$

By using the nondimensional quantities as in Eq. (A.4) and the one for the circumferential stress

$$\bar{\sigma}_\theta=\frac{\sigma_\theta}{E}\left(\frac{pR}{Eh}\right)^{-2/3} \tag{A.15}$$

and from Eqs. (A.13–A.14), the nondimensional governing equations for the circular blister can be obtained as

$$3\bar{w}_{,xx}\bar{w}_{,x}^2+\frac{\bar{w}_{,x}^3}{x}+2\bar{w}_{,xx}\left(\bar{u}_{,x}+\nu\frac{\bar{u}}{x}+(1-\nu^2)\bar{\sigma}_0\right)$$
$$+2\bar{w}_{,x}\left(\bar{u}_{,xx}+\frac{\bar{u}_{,x}}{x}(1+\nu)+(1-\nu^2)\frac{\bar{\sigma}_0}{x}\right)+2(1-\nu^2)=0 \tag{A.16a}$$

$$\bar{u}_{,xx}+\frac{\bar{u}_{,x}}{x}-\frac{\bar{u}}{x^2}+\bar{w}_{,x}\bar{w}_{,xx}+\frac{1-\nu}{2}\frac{\bar{w}_{,x}^2}{x}=0 \tag{A.16b}$$

Eqs. (A.16) can be solved numerically using the method by Kao and Perrone[27] with appropriate boundary conditions. Assuming the membrane is loaded within the elastic range, the energy release rates for the standard and island blister tests can also be determined based on Eq. (A.10) and are given by

$$G=\frac{(pR)^{4/3}}{3(Eh)^{1/3}}\left\{\frac{1}{\pi}\left[5B-\bar{\sigma}_0\frac{\partial B}{\partial\bar{\sigma}_0}\right]-\left(5-\bar{\sigma}_0\frac{\partial}{\partial\bar{\sigma}_0}\right)\right.$$
$$\int_0^1[((\bar{\sigma}_r-\bar{\sigma}_0)^2-2\nu(\bar{\sigma}_r-\bar{\sigma}_0)(\bar{\sigma}_\theta-\bar{\sigma}_0)+(\sigma_\theta-\bar{\sigma}_0)^2)$$
$$\left.+2(1-\nu)\bar{\sigma}_0(\bar{\sigma}_r+\bar{\sigma}_\theta-2\bar{\sigma}_0)]x\,dx\right\} \tag{A.17}$$

for the standard blister, and

$$G=\frac{(pR)^{4/3}}{2a(Eh)^{1/3}}\left\{\frac{1}{\pi}\frac{\partial B}{\partial a}-\frac{\partial}{\partial a}\int_0^1[((\bar{\sigma}_r-\bar{\sigma}_0)^2-2\nu(\bar{\sigma}_r-\bar{\sigma}_0)(\bar{\sigma}_\theta-\bar{\sigma}_0)\right.$$
$$\left.+(\bar{\sigma}_\theta-\bar{\sigma}_0)^2)+2(1-\nu)\bar{\sigma}_0(\bar{\sigma}_r+\bar{\sigma}_\theta-2\bar{\sigma}_0)]x\,dx\right\} \tag{A.18}$$

for the island blister, where a is the nondimensional island radius given by

$$a=\frac{R_{\text{island}}}{R} \tag{A.19}$$

B is the nondimensional blister volume and is given by

$$B=2\pi\int_0^1\bar{w}x\,dx,\quad\text{for the standard blister,}$$

and

$$B=2\pi\int_a^1\bar{w}x\,dx,\quad\text{for the island blister.}$$

It should be noted that the detailed derivation in this section for the circular blisters has been reported in Ref. 23 which contains a different notation convention for nondimensional quantities.

APPENDIX B: CONTRIBUTION OF THE SHEAR FORCE TO THE ENERGY RELEASE RATE

Based on the results in the appendix of Ref. 8, the energy release rate considering shear force contributions in a peel geometry is given by

$$G = [(P - \sigma_0 h)^2 + T^2 + 12M^2/h^2]/2\hat{E}h \tag{B.1}$$

where T is the shear force at the debond front, which is given by

$$T = \sigma_\infty h \sin\theta_\infty \tag{B.2a}$$

P and M at the debond front were given by

$$P = \sigma_\infty h \cos\theta_\infty \tag{B.2b}$$

and

$$M = [\sigma_\infty (1 - \cos\theta_\infty)\hat{E}h^4/6]^{1/2} \tag{B.2c}$$

respectively.

By substituting Eqs. (B.2) into Eq. (1), one can easily find the relative contributions of P, T and M to the energy release rate, which are proportional to $[\cos^2\theta_\infty - 2\sigma_0/\sigma_\infty + (\sigma_0/\sigma_\infty)^2]$, $\sin^2\theta$, and $2(1 - \cos\theta_\infty)/\varepsilon_\infty$, respectively. Table B.1 illustrates the relative magnitudes of these contributions considering the zero prestress case. For most practical cases, the contribution from the shear force is negligible except in the case when the peel angle approaches 90° and the applied peel strain is very large. A similar conclusion can also be easily reached for the non-zero prestress case.

TABLE B.1
Illustration of relative contributions of axial force, shear force, and bending moment to the energy release rate in a peel test

Peel angle, θ	0°	30°	60°	90°	120°	150°	180°
Contribution from P, $\cos^2\theta$	1	0.75	0.25	0	0.25	0.75	1
Contribution from T, $\sin^2\theta$	0	0.25	0.75	1	0.75	0.25	0
Contribution from M, $2(1 - \cos\theta)/\varepsilon_\infty$	0	$0.27/\varepsilon_\infty$	$1/\varepsilon_\infty$	$2/\varepsilon_\infty$	$3/\varepsilon_\infty$	$3.73/\varepsilon_\infty$	$4/\varepsilon_\infty$